

Implication of Nonlinear Kinetics on Risk Estimation in Carcinogenesis

David G. Hoel, Norman L. Kaplan, Marshall W. Anderson

The problem of estimating the risk of cancer resulting from long-term exposure to low doses of a chemical carcinogen is difficult to resolve since there are rarely sufficient data available from humans. An alternative approach to this problem is to estimate low-dose risk in laboratory animals and then extrapolate

only carcinogenic after they have been metabolized, and since nonlinear pharmacokinetics may be involved in the transformation of a chemical into its metabolites, several authors have suggested that tumor response should be related to some measure of metabolite concentration in the target organ rather

Summary. Efforts in estimating carcinogenic risk in humans from long-term exposure to chemical carcinogens have centered on the problem of low-dose extrapolation. For chemicals with metabolites that interact with DNA, it may be more meaningful to relate tumor response to the concentration of the DNA adducts in the target organ rather than to the applied dose. Many data suggest that the relation between tumor response and concentration of DNA adducts in the target organ may be linear. This implies that the nonlinearities of the dose-response curve for tumor induction may be due to the kinetic processes involved in the formation of carcinogen metabolite-DNA adducts. Of particular importance is the possibility that the kinetic processes may show a nonlinear "hockey-stick" like behavior which results from saturation of detoxification or DNA repair processes. The mathematical models typically used for low-dose extrapolation are shown potentially to overestimate risk by several orders of magnitude when nonlinear kinetics are present.

these results to humans. The main disadvantage of this approach is that the exposure levels of interest are so low that an impracticably large number of animals must be used to obtain a reliable estimate. The strategy for circumventing this problem has been to experiment at doses that are much higher than those encountered in the environment, so as to produce tumors at a higher frequency. The results are then extrapolated to the dose levels of interest.

The standard way of doing the low-dose extrapolation has been to assume a parametric model relating applied dose to tumor response, and to use the high-dose data to estimate the model parameters. The choice of model is controversial since various models may adequately fit the data in the experimental range but produce risk estimates at environmental levels that vary by many orders of magnitude (1). Recently, the measure of dose in the dose-response relation has come under discussion (2, 3). Since it is now known that many chemicals are

than to the applied dose (2, 4). In this article we explore two aspects of this issue in detail. First we present relevant biological evidence supporting this point of view, and second we examine the influence on the low-dose extrapolation procedure of the pharmacokinetics involved in the transformation of the chemical into its metabolites.

Biology and the Model

One of the major advances in understanding chemical carcinogenesis was the discovery that most chemical carcinogens are metabolized into a chemically active form (metabolite) that is capable of interaction with many of the cellular macromolecules such as DNA, RNA, and protein (5). Of particular importance are reactions with DNA, since this macromolecule contains the genetic information of the cell.

Data on the mutagenicity of many chemical carcinogens *in vitro* suggest

that mutation results from the cell's attempt at the time of replication to deal with unexcised DNA adducts (covalent interactions of the carcinogen metabolite and DNA). There is also evidence of a linear relation between the concentration of unexcised DNA adducts and the expressible genetic damage. For example, Yang *et al.* (6) examined the induced mutation frequency in normal fibroblasts and XP12BE cells as a function of the number of adducts formed between benzo[*a*]pyrene diol epoxide (BPDE) and DNA in the cells at the time they were released from confluence and plated for the expression of 6-thioguanine resistance. The mutation frequency was linearly related to the BPDE-DNA adduct levels (picomoles per milligram of DNA) at the time the cells were released from confluence. Other investigators have also shown that induced mutation frequencies are linearly related, at least at sublethal doses of the mutagen, to the levels of mutagen-DNA adducts (7, 8). These linear relations suggest that DNA adduct concentrations may be a good measure of the effective biological dose of mutagens in assay systems *in vitro*.

A recent study of transmitted mutations in mice provides additional support for this contention. Russell *et al.* (9, 10) examined the dose-response curve for ethylnitrosourea-induced transmitted mutations in mice. They concluded that the departure from linearity of the dose-response curve at the lower doses is due to the efficient enzymatic removal of the DNA adducts and not to a decrease in the proportion of ingested chemical reaching the testis with decreasing dose.

Various other studies *in vivo* also indicate that concentrations of carcinogen metabolite-DNA adducts in a known target tissue are a good measure of the effective biological dose for initiation of neoplasia.

1) A positive correlation between the carcinogenicity of a series of polycyclic aromatic hydrocarbons (PAH) of widely differing carcinogenic potencies and their extent of reaction with DNA has been observed (11-13). This correlation was not observed with the binding of the reactive metabolite of the PAH to protein and RNA (11, 12). Similarly, the binding of β -propiolactone and other alkylating agents to DNA, but not to RNA

Dr. Hoel is the director of the Biometry and Risk Assessment Program and Dr. Kaplan is a mathematician in the Statistics and Biomathematics Branch, Biometry and Risk Assessment Program, National Institute of Environmental Health Sciences, Research Triangle Park, North Carolina 27709. Dr. Anderson is a Senior Research Scientist in the Molecular and Comparative Pharmacology Section at the Laboratory of Pharmacology, National Institute of Environmental Health Sciences, Research Triangle Park.

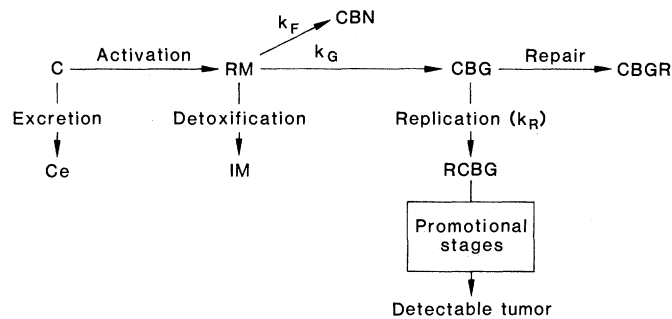
and protein, correlate with their tumor-initiating potency (14). In these studies, total DNA binding (measured as picomoles of radioactivity associated with DNA per milligram of DNA) was used to rank order the carcinogenic potency of the series of carcinogens. Recent studies suggest that levels of specific carcinogen-DNA adducts should be used as a measure of effective dose instead of total DNA binding. For example, for the nitrosamines and nitrosamides, a correlation between carcinogenicity and DNA alkylation has only been observed with O⁶ alkylation of guanine and not with N⁷ alkylation of guanine, even though the latter alkylation is approximately ten times greater than the former (15). Current evidence suggests that the bay-region diol epoxides, such as BPDE, are the ultimate carcinogenic forms for most PAH (16).

2) Recent studies have examined the effect of inhibitors of carcinogenesis on the formation of adducts between carcinogen metabolites and DNA. BPDE-DNA adduct formation and benzo[*a*]pyrene (BP)-induced neoplasia were inhibited to the same degree by butylated hydroxyanisole (BHA) and inducers of aryl hydrocarbon hydroxylase (17, 18). Cohen *et al.* (19) examined the effect of 2,3,7,8-tetrachlorodibenzo-*p*-dioxin (TCDD) treatment on BPDE-DNA adduct formation and BP-induced tumor initiation in the skin of Sencar and CD-mice. BPDE adduct formation in skin was completely inhibited in both strains of mice and BP-initiated papilloma formation was reduced to 7 percent of that in animals not treated with TCDD. Treatment with TCDD also completely inhibited 7,12-dimethylbenzo[*a*]anthracene (DMBA)-induced papilloma formation and DMBA metabolite-DNA adduct formation. In a similar type of study, Swann *et al.* (20) showed that changes in the incidence of DMN-induced kidney tumors produced by changes in the diet and by treatment with BP correspond to the changes these treatments produce in the alkylation of the target tissue DNA by dimethylnitrosamine (DMN).

3) Janss and Benn (21) found a correlation between the amount of DMBA bound to DNA and the incidence of mammary tumors in rats of different ages.

Concentrations of carcinogen-DNA adducts, the rates of removal of these adducts, and the rates of cell turnover may not adequately explain the difference in organ susceptibility and species susceptibility to chemical-induced neoplasia. Promotional aspects of carcino-

Fig. 1. Diagram of a simple pharmacokinetic model for the metabolic fate of some carcinogens. The symbols for the various chemicals are C, nonactivated chemical; RM, reactive metabolite; Ce, excreted chemical; IM, inactive metabolite; CBN, covalent binding, nongenetic; CBG, covalent binding, genetic; CBGR, repaired covalently bound genetic material; RCBG, retained genetic damage, critical and noncritical. In this model, activation, detoxification, and repair are assumed to follow Michaelis-Menten kinetics while the other reactions follow first-order kinetics. The Michaelis-Menten parameters for activation, detoxification, and repair are denoted as (V_M^A, k_M^A), (V_M^D, k_M^D), and (V_M^R, k_M^R), respectively. The symbols for the first-order rate constants are k_F, k_G , and k_R .



genesis might be required to explain these differences. However, this does not detract from the use of carcinogen-DNA adduct levels as a measure of the effective biological dose of the carcinogen in a known target tissue. In particular, for low-dose extrapolation in chemical carcinogenesis, it is thought to be biologically more meaningful to relate tumor response to concentrations of specific DNA adducts in the target tissue than it is to relate tumor response to the administered dose of the chemical. In this article, the concentration of the relevant DNA adduct is referred to as the "effective dose" and is denoted by D^* .

The administered dose is denoted by D .

Relating tumor response to the effective dose is important since the relation between D and D^* could be dose-dependent. In cases when large doses of a chemical carcinogen are administered, metabolic and transport processes could be saturated, leading to a nonlinear relation between the administered and effective doses (2).

The processes involved in transforming a genetically altered cell into a visible tumor are complex. It is therefore unlikely that any simple model will adequately describe these phenomena; consequently, in this article the transforma-

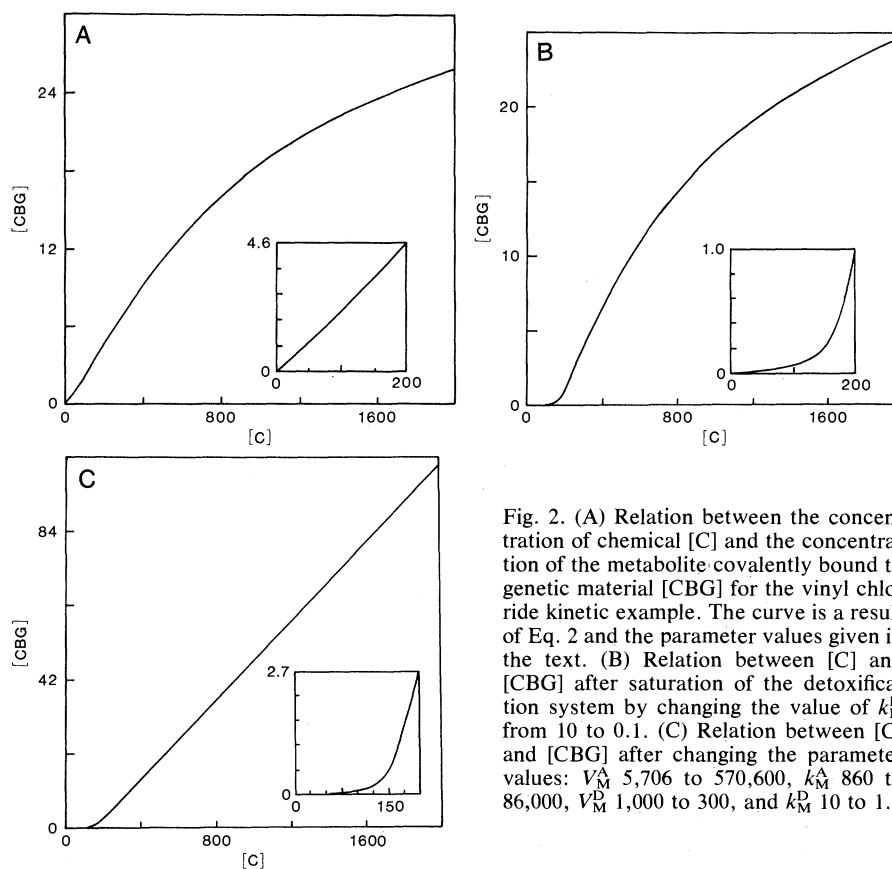


Fig. 2. (A) Relation between the concentration of chemical [C] and the concentration of the metabolite covalently bound to genetic material [CBG] for the vinyl chloride kinetic example. The curve is a result of Eq. 2 and the parameter values given in the text. (B) Relation between [C] and [CBG] after saturation of the detoxification system by changing the value of k_M^D from 10 to 0.1. (C) Relation between [C] and [CBG] after changing the parameter values: V_M^A 5,706 to 570,600, k_M^A 860 to 86,000, V_M^D 1,000 to 300, and k_M^D 10 to 1.

Table 1. Values of the assumed and estimated tumor response derived from the kinetic model in Fig. 2B. For this model, the dose corresponding to a tumor response of 10^{-6} is 0.12, whereas the estimated dose is 0.0024.

| Administered dose | Concentration of CBG | Tumor response* | Estimated response† |
|-------------------|----------------------|-----------------|---------------------|
| 0 | 0.0 | 0.00 | 0.00 |
| 400 | 6.6 | 0.17 | 0.15 |
| 800 | 14.2 | 0.33 | 0.28 |
| 1200 | 19.0 | 0.41 | 0.39 |
| 1600 | 22.3 | 0.47 | 0.48 |
| 2000 | 24.6 | 0.50 | 0.56 |

*Tumor response is assumed to be proportional to the concentration of covalently bound genetic material, CBG. †The estimated tumor response is obtained by statistically fitting a linear-quadratic model to the tumor response plotted against the administered dose.

tion process is regarded as an unknown or "black box." Tumor response, P , can be thought of as some unknown function of D^* , that is, $P = g(D^*)$, and D^* as a function of D , that is, $D^* = f(D)$. The determination of f is essentially a pharmacokinetic exercise, albeit one of great difficulty, but for the sake of discussion it is assumed that it is possible to determine f . The characterization of the function g is quite different. Rather than using ad hoc modeling, simplicity is the motivating force for the choice of g . The simplest choice for g is a straight line, but since P must be between zero and one, $-\log(1 - P)$ is assumed to be a linear function of D^* , that is,

$$P = 1 - \exp[-(a + bD^*)] \quad (1)$$

Adopting this choice for g implies that the nonlinearities that are typically seen in bioassay data are a reflection of the nonlinearities of the kinetic processes involved in converting D to D^* . It should be noted that if D is replaced by D^* , Eq. 1 is identical to that given by the Armitage-Doll model assuming one stage, and the multihit model assuming one hit (I).

A Study of Simple

Pharmacokinetic Models

We now consider some pharmacokinetic models in order to study the behavior of the low-dose risk estimates given by the model proposed in the previous section. The simplest case assumes that all reactions follow first-order kinetics. This implies that D and D^* are proportional, so the risk estimates are the same as those given by the one-hit model and the single-stage Armitage-Doll model. The next level of complexity is demonstrated by the "plateau effect" observed in the dose-response curve for angiosarcomas resulting from exposure to vinyl chloride. The nonlinearity of the dose-response curve is due to the saturation of the activation of the vinyl chloride [see Gehring *et al.* (22)]. For the remainder of

this article we will use a slightly more general kinetic model (see Fig. 1) as developed by Gehring and Blau (2) and studied by Anderson *et al.* (3). This model has the essential features of activation, detoxification, binding, and repair. Furthermore, the compartmental concentrations are represented by a series of simple differential equations. If the exposure concentration is constant and there is rapid distribution to the tissues, the following two steady-state equations describe the relation between the concentration of the nonactivated chemical ($[C]$) and the concentrations of its metabolites in the various pharmacokinetic compartments.

$$k_G[\text{RM}] - k_R[\text{CBG}] - \frac{V_M^R[\text{CBG}]}{k_M^R + [\text{CBG}]} = 0 \quad (2)$$

$$(k_F + k_G)[\text{RM}] + \frac{V_M^D[\text{RM}]}{k_M^D + [\text{RM}]} - \frac{V_M^A[\text{C}]}{k_M^A + [\text{C}]} = 0$$

Since $[\text{RCBG}]$ is proportional to $[\text{CBG}]$, it is sufficient to consider $[\text{CBG}]$ as the effective dose D^* and relate it to $[C]$, provided that $[C]$ is proportional to the administered dose D . This condition is satisfied, for example, when the concentration of the chemical in the blood is proportional to the applied dose and there is rapid diffusion across the cell membrane. In cases when $[C]$ is not proportional to the applied dose, one must obtain the relation between $[C]$ and D explicitly. For the remainder of this article we assume that $[C]$ is proportional to D .

Anderson *et al.* (3) used these equations along with the following estimated parameter values for vinyl chloride: $V_M^A = 5706 \mu\text{g}$ per 4 hours; $k_M^A = 860 \mu\text{g/liter}$; $V_M^D = 1000 \mu\text{g}$ per 4 hours; $k_M^D = 10 \mu\text{g}$ per 0.25 kg; $k_F = 50$ liters per 4 hours; $k_G = 5$ liters per 4 hours; $k_R = 100$ liters per 4 hours; $V_M^R = 100 \mu\text{g}$ per 4 hours; $k_M^R = 70 \mu\text{g}$ per 0.25 kg. In

Fig. 2A the relation between $[C]$ and $[\text{CBG}]$ is given for this set of parameter values. By using this curve, the effective dose values can be obtained corresponding to the doses used by Maltoni and Lefemine (23) in their study of vinyl chloride. Anderson *et al.* (3) used Eq. 1 to obtain an excellent fit of the data of Maltoni and Lefemine. None of the standard statistical models for risk estimation were able to fit these data because all these models predict 100 percent tumor incidence for sufficiently high dose.

It is of interest to study how the shape of the curve in Fig. 2 changes as the kinetic parameters are varied. To investigate this problem, each kinetic parameter was both increased and decreased by two orders of magnitude while the other parameters were kept at their nominal values. This produced 18 plots similar to that in Fig. 2A, except that in a few cases the slope of the curve decreased dramatically as $[C]$ decreased to zero. This gives rise to a curve which departs from linearity at low doses in such a way that the curve has a "hockey-stick" shape. This occurred when the parameters k_M^D , k_F , k_R , and k_M were each reduced in value. The curve for k_M^D is shown in Fig. 2B, which is representative of these four cases. The nonlinear behavior of the curve results from the saturation of the detoxification and repair processes brought on by the reduction of the corresponding Michaelis constant.

To understand the implications of this nonlinear behavior on the low-dose risk estimates, one may consider the following hypothetical example. Suppose that experimental data at $D = 0, 400, 800, 1200, 1600,$ and 2000 are known, where the tumor response frequency is directly proportional to $[\text{CBG}]$. Suppose, also, that the tumor frequency equals 50 percent at the administered dose level of $D = 2000$, that no tumors are observed at the control level $D = 0$, and that only the dose-response of the tumor frequencies at the administered doses are known. Using these data points one can fit a linear-quadratic model

$$P(D) = 1 - \exp[-(\alpha + \beta D + \gamma D^2)] \quad (3)$$

Table 1 shows the fit of the dose-response model in Eq. 3 to the results shown in Fig. 2B where $k_M^D = 0.1$. It is clear from Table 1 that the tumor response is reasonably described by the linear-quadratic model. Next, the dose which corresponds to a "low-risk" tumor frequency of 10^{-6} is compared with the risk estimates generated by the fitted model. For this example, the dose of 0.123 is underestimated to be

0.243×10^{-2} , which reflects the model's inability to detect the nonlinear behavior of the actual dose-response model. Thus, for Fig. 2B, standard methods underestimate the acceptable dose level by a factor of 50.

It is possible to study the effect of the parameter values on the relation between [CBG] and [C] in greater detail by examining the ratio

$$Q(c) = \frac{\left. \frac{d[\text{CBG}]}{d[\text{C}]} \right|_{[\text{C}] = c}}{\left. \frac{d[\text{CBG}]}{d[\text{C}]} \right|_{[\text{C}] = 0}} \quad (4)$$

This ratio measures the relative slopes of the curve relating [CBG] and [C] at values c and 0. If the curve is essentially linear near the origin, then $Q \approx 1$, whereas a large value for Q suggests a hockey-stick appearance. It is convenient to rewrite Q as

$$Q = \frac{1}{(1 + \bar{C})^2} \times Q_1 \times Q_2 \quad (5)$$

where

$$Q_1 = [k_F + k_G + (V_M^D/k_M^D)] / \{k_F + k_G + [V_M^D/k_M^D(1 + \overline{RM})^2]\}$$

$$Q_2 = [k_R + (V_M^R/k_M^R)] / \{k_R + [V_M^R/k_M^R(1 + \overline{CBG})^2]\}$$

and

$$\bar{C} = [C]/k_M^A, \quad \overline{RM} = [RM]/k_M^D, \\ \overline{CBG} = [\text{CBG}]/k_M^R.$$

The circumstances when the ratio Q is large are of interest. Since the quantities Q_1 and Q_2 are always greater than one, Q is large only if Q_1 or Q_2 is large. It is readily demonstrated that Q_1 will be large if

(i) $(V_M^D/k_M^D)/(k_F + k_G)$ is large

and

(ii) \overline{RM} is large.

It follows from Eq. 2 that \overline{RM} will be large if V_M^D/V_M^D is large. These results suggest what parameter conditions produce a hockey-stick shape. In the numerical example this shape was exhibited when either k_M^D or $k_F + k_G$ was small, that is, $(V_M^D/k_M^D)/(k_F + k_G)$ was large. In a similar way one can show that Q_2 is large if

(i) $V_M^R/k_M^R k_R$ is large

and

(ii) \overline{CBG} is large.

A sufficient condition for \overline{CBG} to be large is that $k_M^D k_G/V_M^R$ is large.

These relations suggest which combinations of kinetic parameter values are

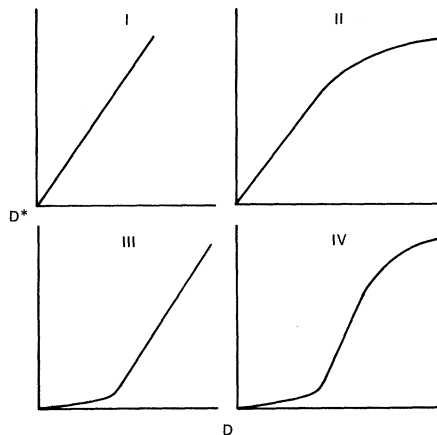


Fig. 3. Possible relations between administered dose D and effective dose D^* for the kinetic model. I, simple first-order kinetics; II, saturation of the activation system; III, saturation of detoxification or repair systems; and IV, combination of II and III.

likely to produce a hockey-stick type of relation between [CBG] and [C], and consequently between tumor response and administered dose. It should be noticed that changing some of the parameters produces conflicting effects on the expressions in Eqs. 6 and 7. For example, V_M^D , V_M^R , k_M^D , and k_G each appear in a numerator and in a denominator in expressions which, if large, imply that Q is large. In contrast, small values of k_F , k_R , and k_M^R suggest large values of Q .

As a final numerical example, let us consider the case where the effect of activation is reduced by increasing V_M^A and k_M^A each by a factor of 100. The hockey-stick shape is obtained by decreasing k_M^D by a factor of 100. The resulting curve relating [CBG] and [C] is shown in Fig. 2C and appears to be perfectly linear for doses above 200. If the tumor response frequency is proportional to [CBG], then there is no possibility of experimentally detecting the low-dose nonlinearity. Furthermore, in this example the dose associated with a low-risk tumor frequency of 10^{-6} is overestimated by a factor of 100.

Both the analytical results and the numerical examples provide some general conclusions:

1) The dose-response curve at low doses may be convex because of saturation of the enzyme systems, although this may be undetected experimentally.

2) The errors in fitting simple dose-response functions tend to overestimate the low-dose effects because of the possible convexity.

3) In no situation did the kinetic model suggest the possibility of undetected concave dose-response behavior leading to an underestimate of low-dose effects.

4) The examples with a hockey-stick shape were linear at low doses and should not be confused with models with a real threshold; that is, there is a positive dose D_0 such that the probability of the biological event occurring at doses below D_0 is zero.

Examples

There are only a few available examples of dose-response data that can be used to test the appropriateness of the approach advocated in this article. There are numerous bioassay data but very few corresponding data relating DNA adduct levels in the target organ to the applied dose. One carcinogen for which such data are available is vinyl chloride. Although the dose-response curve for vinyl chloride provided the first clear example of data that could not be adequately described by existing mathematical models, the model we describe in this article gives an excellent fit to these data (3, 22). Thus the model appears to have greater flexibility in describing dose-response carcinogenesis data.

In Fig. 3, four curves relating D and D^* are presented which can easily be obtained from the pharmacokinetic model of the previous section by an appropriate choice of parameters. In most studies of chemical carcinogenesis, the dose-

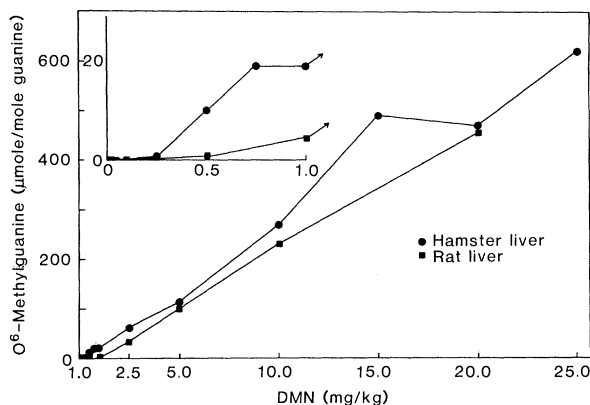


Fig. 4. Amounts of O⁶-methylguanine present in (■) rat and (●) hamster liver DNA 24 hours after administration of DMN. The data are derived from table 1 in Stumpf *et al.* (26) and from Pegg and Hui (27).

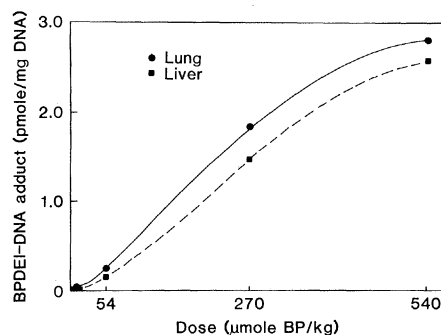
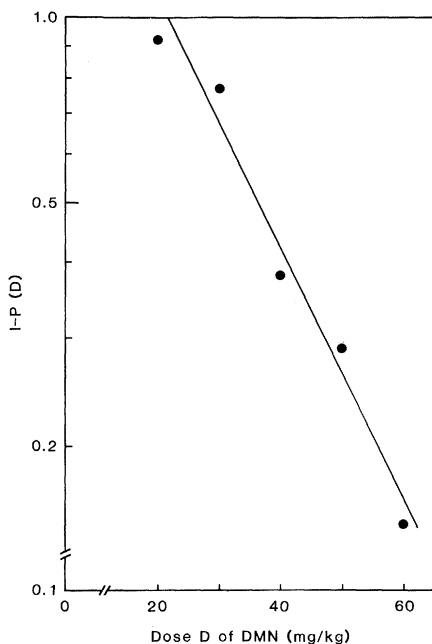


Fig. 5 (left). Graph of $\log[1 - P(D)]$ where $P(D)$ is the probability of kidney tumor 60 weeks after an administration of dose D of DMN. Data are derived from figure 2a of Swann *et al.* (20). Fig. 6 (right). Amounts of BPDE1-DNA adducts present in (Δ) liver DNA and (\bullet) lung DNA of mice that received an oral dose of benzo[*a*]pyrene. The data are derived from Adriaenssens *et al.* (29).

response curves obtained resemble one of the four shapes given in Fig. 3. Thus this model has the ability to fit most, if not all, observed dose-response curves.

Curve III in Fig. 3 is of particular interest since it resembles the dose-response curve one would obtain if there were a real threshold. In a recent study with about 25,000 mice at the National Center for Toxicology Research, the dose-response curve for 2-acetylaminofluorine (2AAF)-induced bladder tumors had a clear hockey-stick shape (24). A recent analysis of the data for 2AAF-induced liver neoplasia also showed that the dose-response curve had a hockey-stick shape (25). The nonlinearities of these dose-response curves may be a consequence of the kinetic processes involved in the formation of 2AAF metabolite-DNA adducts.

There are several examples of dose-response relations for carcinogen metabolite-DNA adducts. Stumpf *et al.* (26) studied the methylation of hamster liver DNA by DMN. The O⁶-methylguanine adduct is considered to be "promutagenic" (15). This adduct appears to be efficiently removed by a methyl transferase (15), but the percentage removed is less when higher doses of DMN are administered. This saturation type of behavior of the repair enzyme produces a clear, nonlinear dose-response curve for O⁶-methylguanine adduct concentrations at specified time points after administration of DMN. Thus, the dose-response curves for O⁶-methylguanine adducts were hockey-stick shaped (Fig. 3, curve III). In contrast the 7-methylguanine adduct levels are linearly related to applied dose (26).

Similar results were obtained with rat liver by Pegg and Hui (Fig. 4) (27). However, higher doses of DMN were required in the rat to produce significant levels of the O⁶-methylguanine adduct. This may account for the appearance of the liver tumors in the hamster but not the rat after a single injection of DMN. Swann *et al.* (20) studied the effect of DMN in rats maintained on a protein-free diet and obtained a hockey-stick shaped dose-response curve for the occurrence of kidney tumors 60 weeks after a single injection of DMN. This can be understood by noting that for large dose values, curve III in Fig. 3 can be approximated by the linear function $D^* = c(D - D_0)$ for $D > D_0$ where D_0 is the hockey-stick's inflection point. From Eq. 1 it then follows that the probability of tumor at dose $D > D_0$ is

$$P(D) = 1 - \exp[-k(D - D_0)]$$

and, consequently, a plot of $\log[1 - P(D)]$ will be a linear function of dose for $D > D_0$. It is clear from Fig. 5 that the data of Swann *et al.* (20) for kidney tumors are consistent with this relation between dose and response.

Several investigators have examined the dose dependency of the formation of BP metabolite-DNA adducts. Pereira *et al.* (28) examined the formation of adducts between BP metabolites and epidermal DNA in mice treated topically with BP. Concentrations of BPDE-deoxyguanosine adducts were linearly related to the applied dose for the dose range examined. Using mice given oral doses of BP, Adriaenssens *et al.* (29) found that the major adduct in the lung and liver was BPDE-deoxyguanosine

and that dose-response curves for the adduct had a hockey-stick shape (Fig. 6), although the shape was not nearly as pronounced as with the O⁶-methylguanine adduct (Fig. 4).

Thus the dose-response curves discussed here for an aromatic amine, a nitrosamine, and a polycyclic aromatic hydrocarbon are consistent with those generated from the kinetic model (Fig. 3). An important conclusion to be drawn from these examples is that in some cases the departure from linearity of the curve for adduct concentration and administered dose can be substantial. Moreover, in those cases where data are available, this nonlinearity appears to be reflected in curves for the applied dose of carcinogen and tumor response.

Conclusion

Although the biological processes in chemical carcinogenesis are complex, there is evidence that for chemicals whose metabolites form DNA adducts, tumor response in laboratory animals is linearly correlated with concentrations of the appropriate DNA adducts in the target organ. We have proposed a simple mathematical model that reflects this phenomenon.

An important implication of this model is that the nonlinearities in the dose-response curves for tumor frequency are attributed to the ongoing kinetic processes involved in the formation of carcinogen-DNA adducts. Studies of some simple models of the kinetic processes show that existing mathematical models can overestimate low-dose risk in instances of nonlinear kinetic behavior.

The relation between the applied dose and the concentration of adduct must be determined before the proposed analysis can be used. One may be able to measure the DNA adduct concentrations directly and so establish the relation between D and D^* . An important benefit of this approach is that the relation between D and D^* can probably be determined at dose levels far below those used in the bioassay.

References and Notes

1. M. D. Hogan and D. G. Hoel, in *Methods in Toxicology*, A. Wallace Hayes, Ed. (Raven, New York, 1982), pp. 711-731.
2. P. J. Gehring and G. E. Blau, *J. Environ. Pathol. Toxicol.* 1, 163 (1977).
3. M. W. Anderson, D. G. Hoel, N. L. Kaplan, *Toxicol. Appl. Pharmacol.* 55, 154 (1980).
4. J. van Ryzin and K. Rai, in *The Scientific Basis of Toxicity Assessment*, H. R. Witschi, Ed. (Elsevier, North-Holland, Amsterdam, 1980), pp. 273-290.
5. E. C. Miller and J. A. Miller, *Cancer* 47, 2327 (1981).
6. L. L. Yang, V. M. Maher, M. McCormick, *Proc. Natl. Acad. Sci. U.S.A.* 77, 5933 (1980).

7. W. E. Fahl, D. G. Scarpelli, K. Gill, *Cancer Res.* **41**, 3400 (1981).
8. R. F. Newbold, P. Brookes, R. G. Harvey, *Int. J. Cancer* **24**, 203 (1979).
9. W. L. Russell, P. R. Hunsicker, G. D. Raymer, M. H. Steele, K. F. Stelzner, H. M. Thompson, *Proc. Natl. Acad. Sci. U.S.A.* **79**, 3589 (1982).
10. W. L. Russell, P. R. Hunsicker, D. A. Carpenter, C. V. Cornett, G. M. Guinn, *ibid.*, p. 3592.
11. P. Brookes and P. D. Lawley, *Nature (London)* **202**, 781 (1964).
12. E. Huberman and L. Sachs, *Int. J. Cancer* **19**, 122 (1977).
13. L. M. Goshman and C. Heidelberger, *Cancer Res.* **27**, 1678 (1967).
14. N. H. Colburn and R. K. Boutwell, *ibid.* **28**, 653 (1968).
15. G. P. Margison and P. J. O'Connor, in *Chemical Carcinogens and DNA*, P. L. Grover, Ed. (CRC Press, New York, 1979), vol. 1, pp. 111-159.
16. R. E. Lehr, H. Yagi, D. R. Thakker, W. Levin, A. W. Wood, A. H. Conney, D. M. Jerina, in *Polynuclear Aromatic Hydrocarbons: Analysis, Chemistry, and Biology*, P. W. Jones and R. I. Freudenthal, Eds. (Raven, New York, 1978), vol. 3, pp. 231-241.
17. A. G. E. Wilson, H. C. Kung, M. Boroujerdi, M. W. Anderson, *Cancer Res.* **41**, 3453 (1981).
18. M. W. Anderson, M. Boroujerdi, A. G. E. Wilson, *ibid.*, p. 4309.
19. G. M. Cohen, W. M. Bracken, R. P. Iyer, D. L. Berry, J. K. Selkirk, T. J. Slaga, *ibid.* **39**, 4027 (1979).
20. P. F. Swann, D. G. Kaufman, P. N. Magee, R. Mace, *Br. J. Cancer* **41**, 285 (1980).
21. D. H. Janss and T. L. Ben, *J. Natl. Cancer Inst.* **60**, 173 (1978).
22. P. J. Gehring, P. G. Watanabe, C. N. Park, *Toxicol. Appl. Pharmacol.* **44**, 581 (1978).
23. C. Maltoni and G. Lefemine, *Ann. N.Y. Acad. Sci.* **246**, 195 (1975).
24. N. A. Littlefield, J. H. Farmer, D. W. Gaylor, *J. Environ. Pathol. Toxicol.* **3**, 17 (1980).
25. K. G. Brown and D. G. Hoel, *Fund. Appl. Toxicol.*, in press.
26. R. Stumpf, G. P. Margison, R. Montesano, A. E. Pegg, *Cancer Res.* **39**, 50 (1979).
27. A. E. Pegg and G. Hui, *Biochem. J.* **173**, 739 (1978).
28. M. A. Pereira, F. J. Burns, R. E. Albert, *Cancer Res.* **39**, 2558 (1979).
29. P. I. Adriaenssens, C. M. White, M. A. Anderson, *ibid.*, in press.

The Economics of Small Farms

Luther Tweeten

Secretary of Agriculture Bob Bergland elevated "structure" to center stage in the farm policy debate during the Carter Administration. The debate dealt with questions of desirable size, number, type, tenure, and legal organization of farms; as well as with market conduct and performance of firms dealt with by farmers in their buying and selling activities (1). The farm structure issue has been muted within the Reagan Administration, but continues among the various publics concerned with agriculture. The issue is likely to reemerge on the future political agenda.

A central issue in the structure debate is the role of the small farm in American agriculture. In this article I take as hypotheses to be tested the following more or less conventional assertions concerning small farms:

- 1) Small farms provide a higher quality of life to operators and their families than do larger farms.
- 2) Small farm operators take better care of their soil than do larger farm operators.
- 3) Small farms are more energy efficient than larger farms.
- 4) Small farm preservation and encouragement avoids the trauma of outmigration of farm people to cities.
- 5) Society would be better off if publicly supported research and extension education were focused on small farms.
- 6) Federal government programs have hastened the demise of small farms.
- 7) Small farms provide the social and

economic support necessary to maintain vitality of nearby towns and cities.

8) Preservation of small farms is essential to economic competition because it avoids concentration of production on a few large farms which would practice monopoly pricing and raise food costs.

The weight of the evidence is brought to bear on each of these hypotheses in the following pages.

For purposes of this analysis, small farms are defined, unless otherwise indicated, as units with crop and livestock receipts of under \$40,000 per year. In 1981, farms with \$20,000 to \$40,000 in sales averaged \$360,000 in assets (excluding dwelling) and about 135 hectares (2). However, assets and hectares vary widely within sales classes from, for example, intensive cattle feedlot operations in the Texas Panhandle to extensive cattle ranching operations in Nevada.

Evaluation of Hypotheses

Small farms provide a higher quality of life. Coughenour and Christenson (3) empirically examined the "small is beautiful" thesis by relating farm size to attitudes about personal well-being, community well-being, and perceived adequacy of community services. They found no evidence that small farmers were more satisfied than large farmers with their personal life, with the social aspects of community life, or with the

social services available to them. Small differences that did emerge from the study suggest that farmers on commercial, family-size units with sales of \$40,000 or more expressed a higher level of perceived well-being than did small-scale farmers.

On the basis of a detailed study of approximately 800 rural families in Iowa and North Carolina from 1970 to 1972, Harper and Tweeten (4) found that income, occupation, education, and age were the principal determinants of personal well-being. Early studies (5) revealed that persons on small, low-income farms were characterized by anomie—feelings of alienation, demoralization, and pessimism. It seems likely that anomie prevalent on small farms is more the product of low income than of small farm size per se. Able-bodied, full-time operators of small farms have a high incidence of low income, and it is difficult to separate positive feelings of independence and pride of ownership of a small farm from negative feelings arising from poverty and underemployment. Small farms with sales of \$20,000 to \$40,000 per year received operator-family labor income from farming that averaged less than \$4000 per year from 1975 to 1981; smaller farms received even less.

If full-time small farms are providing a low quality of life, we should observe a mass exodus from these farms or a shift of operators from full-time to part-time status. That adjustment is precisely what we observe in Fig. 1, which shows trends for U.S. farms with sales of \$2500 to \$20,000 per year (6). The upper graph indicates that continuation of the 1959-1969 or 1959-1974 trends would leave no full-time, able-bodied small farm operators by the early 1980's. With stability or growth in numbers of small farms with aged operators (lower graph) and part-

The author is Regents Professor, Department of Agricultural Economics, Oklahoma State University, Stillwater 74078.